Bioconjugate Chemistry

Communication

Cite This: *Bioconjugate Chem.* 2019, 30, 2998−3006

pubs.acs.org/bc

Interactions between PHD3-Bromo of MLL1 and H3K4me3 Revealed by Single-Molecule Magnetic Tweezers in a Parallel DNA Circuit

Xiaofeng Ma,[†] Manning Zhu,[†] Jianyu Liu,[‡] Xu Li,[†] Lihua Qu,[†] Lin Liang,[†] Wei Huang,[†] Junli Wang,[†] Ning Li,[†] Jun-Hu Chen,[*,§] Wenke Zhang,[*,‡] and Zhongbo Yu[*,†]

[†]State Key Laboratory of Medicinal Chemical Biology, College of Pharmacy, Nankai University, 38 Tongyan Rd, Tianjin 300353, China

[‡]State Key Laboratory of Supramolecular Structure and Materials, College of Chemistry, Jilin University, Changchun 130012, China

[§]National Institute of Parasitic Diseases, Chinese Center for Disease Control and Prevention, WHO Collaborating Center for Tropical Diseases, National Center for International Research on Tropical Diseases, Key Laboratory of Parasite and Vector Biology, Ministry of Health, Shanghai 200025, China

Supporting Information

ABSTRACT: Single-molecule force spectroscopy is a powerful tool to directly measure protein−protein interactions (PPI). The high specificity and precision of PPI measurements made it possible to reveal detailed mechanisms of intermolecular interactions. However, protein aggregation due to specific or nonspecific interactions is among the most challenging problems in PPI examination. Here, we propose a strategy of a parallel DNA circuit to probe PPI using single-molecule magnetic tweezers. In contrast to PPI examination using atomic force microscopy, microspheres as probes used in magnetic tweezers avoided the single-probe issue of a cantilever. Negatively charged DNA as a linker circumvented the severe aggregation in the PPI construct with a protein linker. The unnatural amino acid encoded in proteins of interest expanded the choices of biorthogonal conjugation. We demonstrated how to apply our strategy to probe the PPI between the PHD3-Bromo and the histone H3 methylated at K4, a critical epigenetic event in leukemia development. We found a rupture force of 12 pN for breaking the PPI, which is much higher than that required to peel DNA off from a nucleosome, 3 pN. We expect that our methods will make PPI measurements of mechanics and kinetics with great precision, facilitating PPI-related research, e.g., PPI-targeted drug discovery.

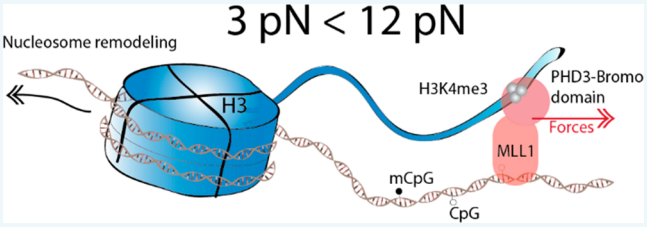

Protein−protein interactions (PPI) are fundamental in broad fields, e.g., research of drug targets.[1,2] Single-molecule technologies provide powerful methods to specifically and precisely probe PPI. For example, the PPI of cohesin-dockerin has recently been directly measured using atomic force microscopy (AFM).[3,4] In force-ramp assays of AFM, cohesin on a cantilever searched and bound a dockerin on a surface, giving a PPI signal upon a rupture event. Alternative strategies with a flexible linker also emerged to investigate intramolecular or intermolecular interactions in single-molecule manipulations on proteins.[5] A mechanical circuit in series for intramolecular PPI examination used a flexible and unstructured protein linker of 182 amino acids which was fused between the two protein domains of interest.[6,7] PPI signal came from the release of the unstructured linker when forces broke PPI. A mechanical circuit in parallel was recently developed, which used a flexible linker of a third protein to connect a pair of proteins, allowing direct identification of intermolecular PPI using AFM.[8] The dissociation of intermolecular PPI gave a signal of increasing contour length because forces extend the flexible linker. The flexible protein linker was conjugated to the polyprotein handles via disulfide bonds, while the proteins for PPI examination were fused with polyprotein handles.

Protein aggregation due to specific or nonspecific interactions is among the most challenging problems in PPI examination.[2] AFM uses one cantilever at a time to search PPIs. Protein A on the single probe can be easily blocked by binding of protein B detached from the surface, resulting in failed detection. For the strategy of the protein circuit in parallel, the protein handles and linkers potentially underwent nonspecific aggregation due to the complicated surface charges. Besides, the length of protein handles and linkers had limitations due to the difficulties in expressing big proteins. Moreover, conjugating sites were also extremely limited because of the few choices of proper functional groups in natural amino acids.

Herein, we propose a strategy of a parallel DNA circuit to probe PPI using single-molecule magnetic tweezers. Thousands of microspheres in a typical assay of magnetic tweezers

Received: October 2, 2019
Revised: November 9, 2019
Published: November 12, 2019

Downloaded via NANKAI UNIV on December 26, 2019 at 08:29:53 (UTC).
See https://pubs.acs.org/sharingguidelines for options on how to legitimately share published articles.

© 2019 American Chemical Society

DOI: 10.1021/acs.bioconjchem.9b00665
Bioconjugate Chem. 2019, 30, 2998−3006

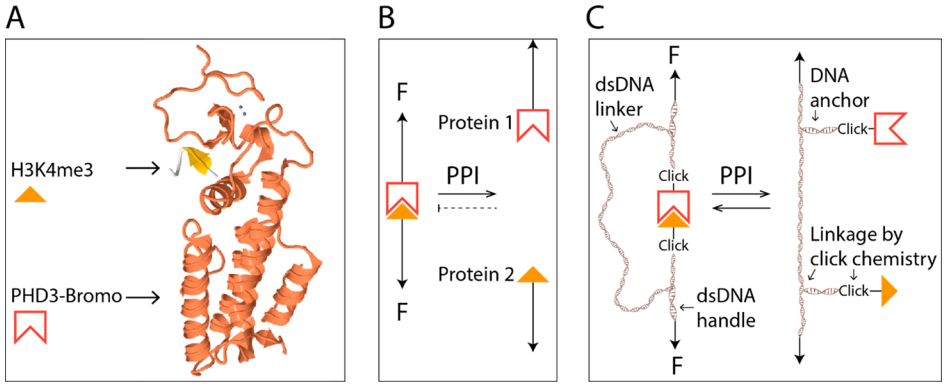

Figure 1. Single-molecule strategies to examine the mechanics of PPIs. (A) Structure of MLL1 PHD3-Bromo domain binding H3K4me3 of trimethylated H3 tail (PDB 3LQJ). (B) Rupture of PPIs one pair at a time by forces. (C) Repetitive examination of PPIs using a mechanical circuit in parallel assisted by dsDNA as handles and a flexible linker. Two dsDNA handles flank the linker dsDNA for mechanical manipulation. Two DNA anchors bifurcate out at both sides of the linker DNA for protein conjugation. Proteins of interest carry UAA with clickable groups. Bioconjugation between proteins of interest and DNA handles are via click chemistry.

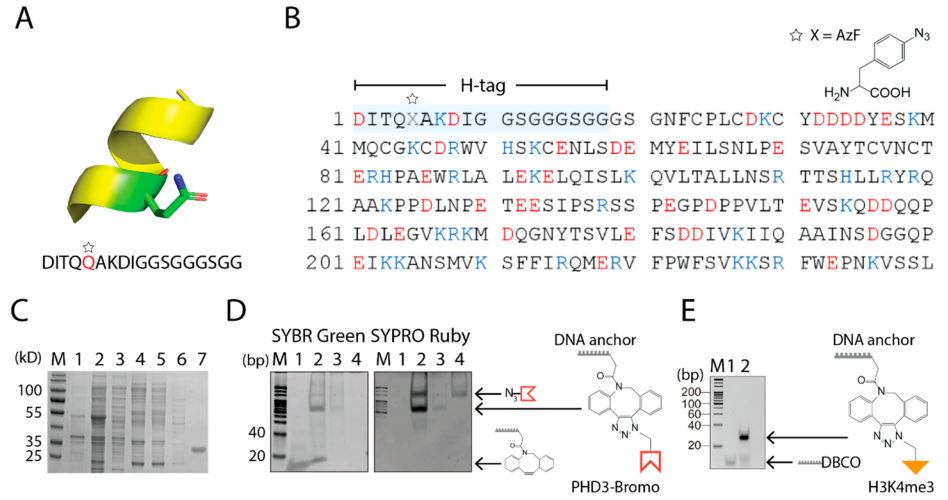

Figure 2. Bioconjugation of DNA and the PHD3-Bromo with an H-tag, as well as H3K4me3. (A) Structure and sequence of H-tag from pfRON2 (PDB: 3ZWZ). The fifth amino acid of Q (Star) is highlighted in the structure for harboring the UAA of AzF. (B) Sequence of PHD3-Bromo with H-tag at the N-terminus. The X (Star) at the fifth position is for the mutagenesis of AzF. Blue and red colors indicate positive and negative charges, respectively. (C) Expression and purification of H-tagged PHD3-Bromo. M: protein marker. Lane 1: supernatant. Lane 2: pellet. Lane 3: flow through. Lanes 4−6: wash. Lane 7: PHD3-Bromo with H-tag. (D) Bioconjugation between H-tagged PHD3-Bromo and DNA via click chemistry. The same gel showed both nucleic acids (SYBR Green) and proteins (SYPRO Ruby). M: DNA marker. Lane 1: DBCO modified DNA. Lane 2: products after click reaction. Lane 3: conjugation product of DNA−protein after purification. Lane 4: H-tagged PHD3-Bromo with AzF. (E) Bioconjugation between H3K4me3 and DNA via click chemistry. M: DNA marker. Lane 1: DBCO modified DNA. Lane 2: products of click reaction.

served as probes, avoided the single probe issue in AFM. DNA evenly carries negative charges, reducing the aggregation issue of the PPI construct. Unlike protein, the length of DNA handles and linkers is easily scalable using general methods of molecular biology. We genetically modified proteins with unnatural amino acids (UAA), allowing bioconjugation with DNA handles via click chemistry. The UAA encoded in the proteins of interest expanded the choices of biorthogonal conjugation, which cracked the limits of available functional groups in natural amino acids. In the mechanical circuit, a long DNA serves as a flexible linker which is parallel with the short PPI branch. Upon a rupture event of the PPI by forces, the flexible DNA linker restrains the diffusion of the proteins and makes the next experiment of PPI convenient. We demonstrated how to apply our strategy to probe the PPI between the PHD3-Bromo domain of human MLL1 protein and the tail of histone H3 methylated at K4 (H3K4me3).[9] The PHD3-Bromo domain, a drug target, recognizes the methylated H3 tail which can be modified by the MLL1 SET domain.[9−11] On the other hand, the MLL1 CXXC domain binds DNA at CpG sites.[12,13] Chromatin remodeling slides DNA around a nucleosome, generating complex mechanical environment for MLL1.[14] We found a rupture force of 12 pN for breaking the PPI between PHD3-Bromo and H3K4me3, which is much higher than that required to peel DNA off from a nucleosome, 3 pN. Elucidating the mechanical interactions of MLL1 binding a histone tail could help to understand the epigenetic regulation under chromatin dynamics.[15,16]

RESULTS

We designed a strategy of PPI measurement using single-molecule force spectroscopy. As an epigenetic enzyme, MLL1 contains multiple domains interacting with both DNA and histones, e.g., CXXC domain binding CpGs on DNA and

DOI: 10.1021/acs.bioconjchem.9b00665
Bioconjugate Chem. 2019, 30, 2998−3006

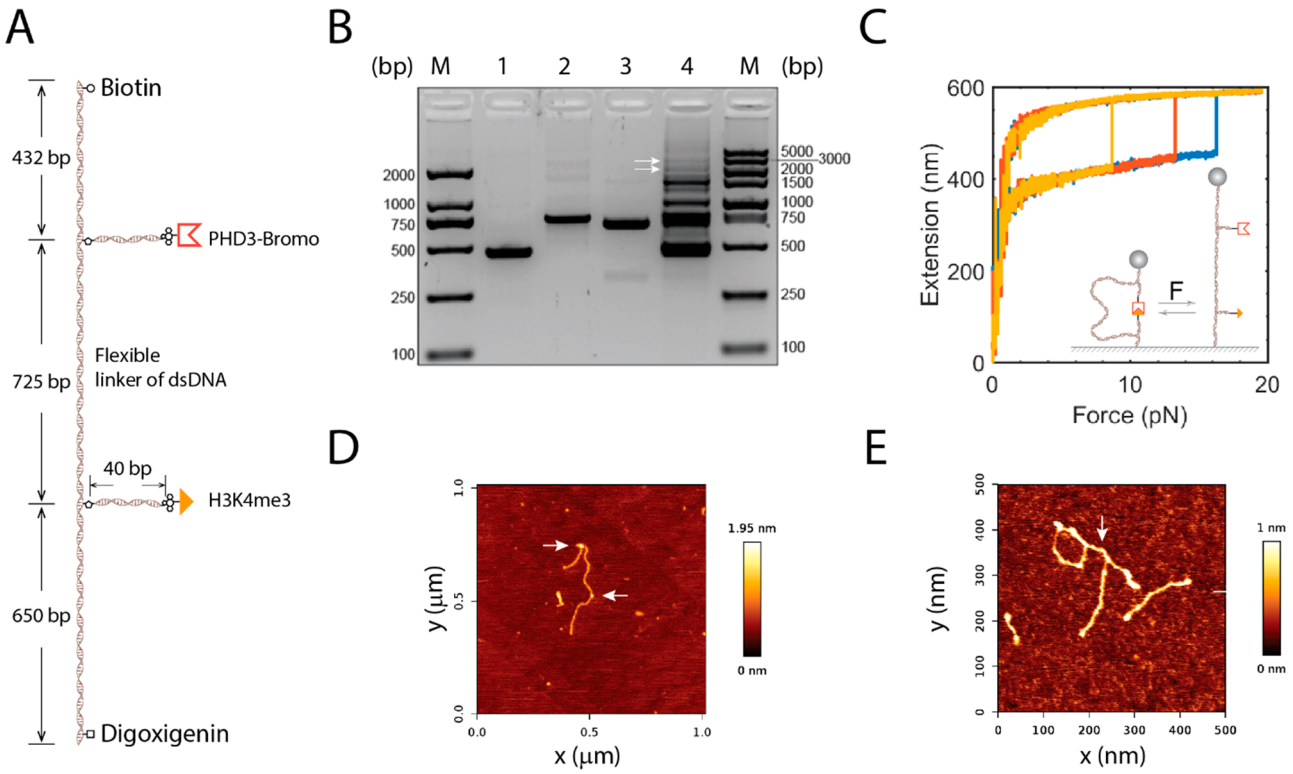

Figure 3. PPI construct validated by gel, magnetic tweezers, and AFM imaging: (A) PPI construct designed for H-tagged PHD3-Bromo and H3K4me3. (B) Agarose gel showed the ligation products of the PPI construct. M: DNA marker. Lane 1: DNA handle of 432 bp anchored with H-tagged PHD3-Bromo. Lane 2: DNA linker of 725 bp. Lane 3: DNA handle of 650 bp with H3K4me3. Lane 4: ligation products. Arrows indicate the PPI constructs in either closed conformation (Top) or linear conformation (Bottom). (C) Force–extension curves showed three PPI breaking signals collected on single-molecule magnetic tweezers. Three traces were from the same molecule in a Tris (pH 8) buffer with 100 mM NaCl. (D) AFM imaging showed a PPI construct in a linear conformation. Arrows indicate the positions of PHD3-Bromo (Top) and H3K4me3 (Bottom). (E) AFM imaging showed a PPI construct in a closed structure. Arrow pointed the predicted position of PPI, measured from the two ends of the construct.

PHD3-Bromo domain reading triple-methylated lysine (K4me3) in the histone H3 tail.[11,13] The PPI between PHD3-Bromo and H3K4me3 tail must encounter mechanical forces upon chromatin activities, such as nucleosome remodeling and MLL1-coordinated transcription of hoxa9 gene.[17−19] The mechanical forces to break the PPI between PHD3-Bromo and H3K4me3 should be weak enough for MLL1 to organize chromatin dynamically. Although single-molecule force spectroscopy, especially magnetic tweezers and optical tweezers, is powerful to measure weak forces, we need a PPI construct for sensitive, specific, and convenient measurements to understand the intermolecular mechanics.

Taking MLL1 PHD3-Bromo and H3K4me3 tail as an example, we designed a parallel DNA circuit to probe the protein−protein interactions mechanically. The crystal structure of the PHD3-Bromo complex with the H3(1-9)K4me3 peptide of 9 amino acids (ART(Kme3)QTARK) showed that H3K4me3 binds PHD3 (Figure 1A).[9] In our design, orthogonal bioconjugation between DNA handles and proteins formed a parallel circuit, allowing convenient force manipulation in a repetitive manner (Figure 1B vs C). Two proteins, anchored to DNA handles, aligned along the axis of forces upon PPI formation. The branch of flexible dsDNA linker and the PPI branch formed the mechanical circuit in parallel (Figure 1C). Because the anchoring DNA were as short as 40 bp in length, the flexible dsDNA linker of >700 bp experienced negligible forces than that on the PPI branch. When forces broke PPI, the dsDNA linker became straight along DNA handles to experience all the forces. Meanwhile, proteins held zero forces and dangled from the DNA handles via the DNA anchors. By manipulating forces, single-molecule force spectroscopy can repeatedly probe the PPI formation and breakage in this parallel DNA circuit. We used click chemistry to achieve the orthogonal bioconjugation between proteins and DNA anchors, as well as that between DNA anchors and DNA handles.

To achieve orthogonal bioconjugation via click chemistry between PHD3-Bromo and DNA, we incorporated a UAA of *p*-azidophenylalanine (AzF) into the protein. Previous research revealed that residue choice influences the efficiency of bioorthogonal protein conjugation.[20,21] As a rule of thumb, good residue choices are in a structure of α-helix and neutral local polar environment, not charged and not extremely exposed or buried but moderately accessible on a surface. Among the tested proteins in our lab, we found a peptide of 18 amino acids from RON2 (*Plasmodium falciparum*) to harbor an AzF, which satisfies the rules, forms α-helix, and keeps AzF highly reactive (Figure 2A).[22] We placed the RON2 peptide at the N-terminus of PHD3-Bromo, called "H-tag". The fifth Q in the H-tag is the mutation site for AzF (X), which is flanked by a polar uncharged amino acid of Q and a hydrophobic amino acid of A (Figure 2B). The side chain of AzF sticks out of the α-helix of H-tag, relatively far from any charged amino acids around.

We genetically incorporated the UAA of AzF (Figure 2B) into the PHD3-Bromo domain of the MLL1 protein in

DOI: 10.1021/acs.bioconjchem.9b00665
Bioconjugate Chem. 2019, 30, 2998−3006

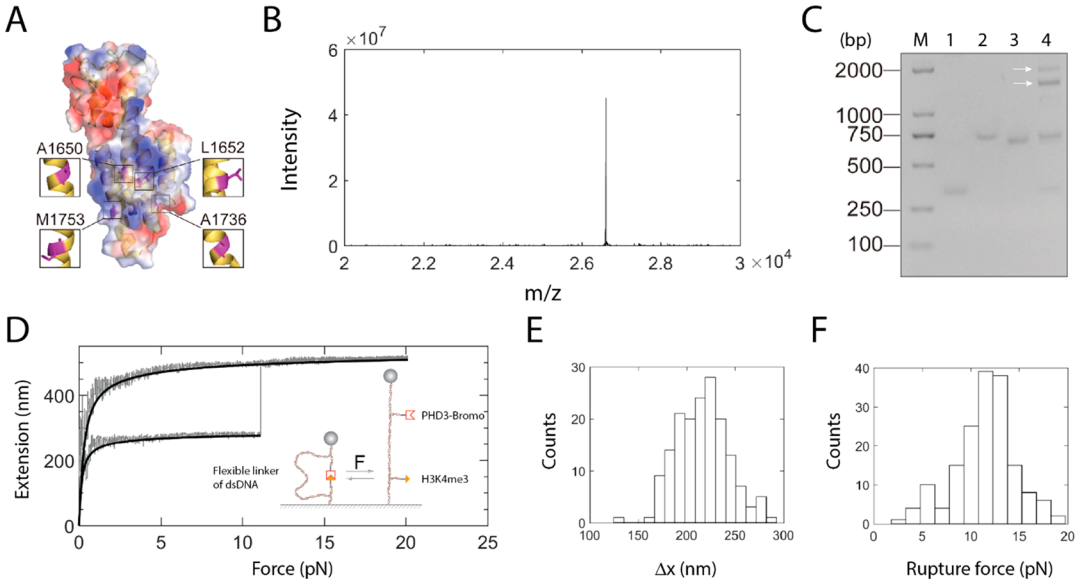

Figure 4. Mechanics of PPI between PHD3-Bromo and H3K4me3 revealed by a DNA circuit in parallel. (A) Illustration of tested sites in the PHD3-Bromo structure (PDB 3LQH) to incorporate AzF with an amber stop codon considering the surface nanoenvironment. Zoom in for the second structures of mutating sites. Blue, red, and white for positive, negative, and neutral charges, respectively. (B) Mass spectrometry validated the successful incorporation of AzF into PHD3-Bromo (M1753 as an example). (C) Agarose gel showed the assembled DNA circuit in parallel. Two arrows indicated the PPI construct in a closed conformation (Top) or a linear conformation (Bottom). M: DNA marker. Lane 1: DNA handle at the PHD3-Bromo side. Lane 2: flexible DNA linker. Lane 3: DNA handle at the H3K4me3 side. Lane 4: ligation products. (D) Force−extension trace of stretching and relaxing the mechanical circuit in parallel using single-molecule magnetic tweezers. The abrupt leap at 11 pN indicated a rupture event of the complex formed by a PHD3-Bromo and an H3K4me3 in a PBS buffer (pH 7.4). The solid black lines represent Worm-Like-Chain fitting. (E) Histogram of changes in extension upon rupture events (N = 167 events out of 22 molecules). (F) Histogram of rupture forces (N = 167 events out of 22 molecules).

Escherichia coli. Clickable UAA is popular in bioconjugation reactions for protein cross-linking and fluorophore labeling.[23−25] Genetically encoded UAA, taking advantage of orthogonal aminoacyl-tRNA synthetase/tRNA pairs, is a powerful tool for protein−DNA conjugation using click chemistry.[21,26] The employed pair of aminoacyl tRNA synthetase/tRNA recognizes an amber stop codon (TAG)[27] (Figure S1). SDS-PAGE analysis revealed that full-length proteins were produced in the presence of 1 mM AzF (Figure 2C). We purified the expressed protein of H-tagged PHD3-Bromo with a purity of >95% (Figure 2C).

To construct the PPI branch of the parallel circuit, we used copper-free and strain-promoted alkyne−azide cycloaddition (SPAAC) to achieve biorthogonal conjugation between a dibenzylcyclooctyne(DBCO) functionalized ssDNA anchor and the side chain of AzF in PHD3-Bromo (Table S1). Using two fluorescent dyes, we examined nucleic acid, protein, and the conjugates in the same gel, which showed >50% of the conjugating efficiency (Figure 2D). We also conjugated a DBCO-modified ssDNA anchor to an azide-modified H3K4me3 using SPAAC (Figure 2E). We avoided copper to make the click reaction less toxic to our proteins.

Using the conjugates of H-tagged PHD3-Bromo and H3K4me3 on DNA anchors, we made the PPI construct in a parallel DNA circuit with a flexible linker. We ran Cu(I)-catalyzed azide−alkyne cycloaddition (CuAAC) to conjugate azide and alkyne modified DNA, which produced bifurcated oligos ($P^{\perp}$ or $H^{\perp}$) (Figure S2). One arm of the bifurcated oligos serves as an anchor to carry proteins of interest. The other arm of the bifurcated oligos serves as a primer in the PCR reaction to produce dsDNA handles that flank at the two sides of a flexible dsDNA linker of 725 bp (Figure 3A). Biotin and digoxigenin modifications on DNA handles allowed affinity immobilization of the PPI construct on functionalized surfaces for mechanical manipulation. The handles at the biotin or digoxigenin ends were 432 bp or 650 bp, respectively. We examined the construction of the parallel DNA circuit using agarose gel electrophoresis (Figure 3B). In lane 4, we saw two bands (top:bottom = 0.85:1) at the expected position for the PPI construct (Arrows in Figure 3B). Because nicked circular DNA migrates more slowly than linear ones in an agarose gel,[28,29] we rationalized that PPI between PHD3-Bromo and H3K4me3 closed the DNA circuit, forming a circular conformation (top arrow). On the other hand, the open circuit was in a linear structure (bottom arrow). Agarose gel thus revealed the successful construction of the DNA circuit.

We next used single-molecule magnetic tweezers to probe PPI of PHD3-Bromo and H3K4me3 in the parallel DNA circuit. The splint DNA of 40 bp supports the PPI branch of the mechanical circuit to afford 65 pN in the shear geometry, which is identical to that of dsDNA melting forces.[30] The 1,2,3-triazole resulting from click chemistry can afford up to 860 pN and split into an alkyne and an azide,[31] which is sufficiently strong to probe PPIs at a range of tens of piconewtons in our single-molecule mechanical assays. The two ends of DNA handles carry digoxigenins and biotins, respectively, immobilizing the parallel circuit between a glass slide covered by the anti-digoxigenin antibody and a magnetic bead coated with streptavidin through affinity interactions (Figure 3C, cartoon). A pair of permanent magnets generate forces to the proteins of interest in the DNA circuit by providing a horizontal magnetic field and manipulating the bead in the vertical direction. At a force loading rate of ±4 pN/

DOI: 10.1021/acs.bioconjchem.9b00665
Bioconjugate Chem. 2019, 30, 2998−3006

s, we repetitively ran force-ramp assays to stretch and relax the parallel circuit between 0 pN and 20 pN.

The extension of the construct underwent two trajectories. The sharp transitions manifested the rupture events of PPIs between PHD3-Bromo and H3K4me3 (Figure 3C). Before rupturing, the parallel circuit held by PPI followed the short trajectory when pulled by forces. Upon rupture, PPI broke and released the flexible DNA linker, generating a sharp transition from the short trajectory to the long one at the rupturing force. Abrupt transitions of 139 ± 15 nm happened at 12 ± 4 pN (mean and sd, n = 22 from 3 molecules) in a Tris (pH 8) buffer with 100 mM NaCl. Considering the end-to-end distance contributed from the PPI branch, especially two DNA anchors of 80 bp, the 18 amino acids of H-tag, and the geometry of PHD3-Bromo binding H3K4me3, the difference between the short and long trajectories extracted from the PPI signals was close to the release of the flexible DNA linker at 12 pN. For a single molecule, over 70 measurements of force ramp assays at a subsequent time interval of a few seconds, we observed 20 PPI signals, giving an occurrence of 29%. The single-molecule manipulation validated the successful construction of a parallel circuit for PPIs and revealed the mechanics of interactions between PHD3-Bromo and H3K4me3.

We further examined the PPI construct of H-tagged PHD3-Bromo using AFM imaging. On a mica surface, adsorption of the PPI construct at a proper geometry could reveal the anchoring sites of PHD3-Bromo and H3K4me3 on DNA. We found two high spots at different sizes on a DNA molecule (Figure 3D). According to the molecular weight, we recognized the large spot as the H-tagged PHD3-Bromo of 240 amino acids (Top arrow). The small spot was the H3K4me3 of 9 amino acids (Bottom arrow). The H-tagged PHD3-Bromo was at the side of a short DNA handle with biotin. The H3K4me3 was at the side of a long DNA handle with digoxigenin. The measured length was consistent with the theoretical calculations, 147 nm for the short handle of 432 bp and 221 nm for the long handle of 650 bp. Moreover, we observed the closed conformation of PPI construct (Figure 3E). Based on the measurements from the ends of the DNA handles, we found that the DNA circuit tangled at the site of PPI between H-tagged PHD3-Bromo and H3K4me3 (Arrow). AFM imaging corroborated the results of agarose gel electrophoresis and single-molecule magnetic tweezers, validating the successful construction of the DNA circuit in parallel for PPI investigation.

H-tag could potentially affect the measurements of PPI between PHD3-Bromo and H3K4me3. To rule out the influence of H-tag, we made a PPI construct with the UAA of AzF directly incorporated inside the PHD3-Bromo sequence. The residue choice for genetical incorporation of UAA into PHD3-Bromo dramatically affected the bioconjugation efficiency via click chemistry. Following the rules of residue choices,[9,20] we tested four sites in PHD3-Bromo (A1650, L1652, A1736, and M1753) regarding surface accessibility, secondary structure, residue charge, and local environment (Figure 4A). After expression and purification of the four PHD3-Bromo with AzF, we confirmed the expression of proteins using Western blot (Figure S3). We found that the reaction efficiency of click chemistry between PHD3-Bromo and oligonucleotides was 14% (A1650AzF), 9% (L1652AzF), 7% (A1736AzF), and 5% (M1753AzF) (Figure S4). We chose PHD3-Bromo (A1650AzF) with the highest reaction efficiency to make the mechanical parallel circuit for probing PPIs. Q-TOF-MS further validated the successful incorporation of AzF in PHD3-Bromo (Figure 4B). Agarose gel showed two bands of the PPI construct (top:bottom = 0.75:1), which were circular and linear structures, like that of H-tagged construct (Figure 4C).

We examined the PPI construct without H-tag using single-molecule magnetic tweezers. Under similar experimental conditions as used previously, we observed PPI signals in force-ramp assays (Figure 4D). The extension of the PPI construct followed the Worm-Like-Chain model when forces increased or decreased (Figure 4D, solid black lines). The rupture events of PPIs between PHD3-Bromo and H3K4me3 revealed changes in extension of 214 ± 26 nm at a critical force of 12 ± 2 pN in a PBS (pH 7.4) buffer (mean and sd, n = 167, Figure 4E and F). The dimensional difference between the short and long paths measured from the transition signals agrees well with the length of the flexible DNA linker, 218 nm for 733 bp at 12 pN. The rupture forces for both H-tagged construct and the one without H-tag were identical, 12 pN, indicating that H-tag has no influence on the mechanics of PPI between PHD3-Bromo and H3K4me3.

DISCUSSION

We have developed a mechanical circuit with a flexible linker of dsDNA conjugating a pair of proteins in parallel to probe PPIs. UAA assisted conjugation circumvents the considerable mutagenesis frequently happening in the cysteine-based protein engineering. Although click chemistry is a convenient method for bioconjugation[32,33] and has been used in single-molecule force spectroscopy,[34−37] the examination of PPIs has rarely used orthogonal conjugation between proteins of interest and DNA handles in a mechanical circuit. Because the residue in the protein to genetically encode a UAA should be optimized on a case by case basis to achieve a satisfying efficiency for orthogonal conjugation, we developed an H-tag strategy to harbor the UAA, avoiding the optimization issue. On the other hand, the available UAA sites in a protein for orthogonal conjugation make it possible to stretch PPIs in multiple defined directions mechanically. In contrast to isothermal titration calorimetry and surface plasmon resonance, information on thermodynamics and kinetics resulting from multiple directions of single-molecule mechanical manipulation will allow the construction of complex energy landscapes of PPIs in three dimensions, which have been achieved in folding studies of a protein structure or a high-order DNA structure.[35,38−40]

Protein aggregation is another challenging issue in PPI examination. Interactions among PPI constructs can quickly go to a high order, making the direct measurement of single molecules difficult. AFM has been used to probe PPI in a parallel circuit with a flexible protein linker.[8] Extra care should be taken to rule out PPI signals from aggregation events. In this work, magnetic tweezers use microspheres to probe PPI. Applying strong forces, we can conveniently break tethers of aggregates and pull microspheres off from the field of view under a microscope. By picking up single microspheres at the expected high, one can easily find single molecules of the PPI construct. Taking advantage of the sensitivity of single-molecule magnetic tweezers, we can probe PPI at a low concentration which helps to decrease protein aggregation. In 40 μL of reaction volume, we routinely mixed 10 μL of M270 beads with 0.1 ng of the PPI construct, calculated according to

DOI: 10.1021/acs.bioconjchem.9b00665
Bioconjugate Chem. 2019, 30, 2998−3006

the DNA of ~2 kb. Our method can thus conquer the protein aggregation issue in PPI investigation.

We avoided harsh conditions for proteins in the preparation of the PPI construct. For example, we avoided precipitation steps or high temperatures when handling proteins of interest. We used electroelution to recover conjugates out of gel pieces. Buffer changing relied on dialysis or filter devices. AFM revealed that single-molecule dispersion of the PPI construct after lyophilization is hard due to aggregation (data not shown). We used a filter device to condense the PPI constructs.

The designed handles and linker with dsDNA make the mechanical parallel circuit easily scalable for both length and number of branches. A long and flexible linker had a negligible effect on the PPI of interest, allowing precise measurement of the rupture forces. On the other hand, DNA stiffness could be adjusted by changing the length.[41,42] A DNA linker of various sizes in the parallel circuit may serve as a tool to mechanically modulate PPI.

Our method revealed the rupture force of 12 pN between PHD3-Bromo and H3K4me3. The rupture force is much stronger than 3 pN, which is required to peel DNA off from a nucleosome.[19,43,44] Such strong PPI between MLL1 and nucleosome assures the binding during nucleosome remodeling.[17,18,45] Mechanical forces could thus serve as a regulating mechanism in nucleosome-related activities of MLL1. For the PPI construct of H-tagged PHD3-Bromo, we observed 46% of the PPI formation in gel electrophoresis and 29% in single-molecule assays using magnetic tweezers. The discrepancy could be explained by PPI forming kinetics. Gel result of 46% showed PPI formation at equilibrium, while magnetic tweezers with 29% revealed PPI signals at a nonequilibrium state. By changing the time intervals between two subsequent force-ramp assays, we could further examine the detailed kinetics of PPI formation. In addition, we could measure the kinetics of PPI dissociation using force-jump assays. It would also be interesting to apply our method to measure the rupture forces and kinetics between MLL1 PHD3-Bromo and histone H3 with different methylation levels at K4, i.e., 0−3 methyl groups. We expect that our single-molecule method using the parallel DNA circuit will make PPI measurements more convenient with high precision, facilitating PPI-related research, e.g., PPI-targeted drug discovery.

METHODS

Other than expressly noted, we have purchased all chemicals from Sigma-Aldrich and enzymes from New England Biolabs.

Expression and Purification of MLL1 PHD3-Bromo with Azide-Phenylalanine. We used two strategies to genetically incorporate a UAA into the PHD3-Bromo domain of MLL1 protein. The first strategy employed a peptide of 18 amino acids (DITQXAKDIGGSGGGSGG) in which X represented the UAA (Table S1).[22] Because the peptide can form a structure of α-helix, providing an environment for the UAA to remain highly active in the reaction of click chemistry, we called the peptide H-tag. We fused the H-tag at the N-terminus of PHD3-Bromo. In the second strategy, we directly incorporated a UAA in the sequence of PHD3-Bromo (Table S1), where the click chemistry reaction showed high efficiency. Other than the difference of protein sequences between the two strategies, the expression and purification protocols were similar. We next described the steps of protein expression and purification using the second strategy as an example.

From professor Zhanxin Wang (Beijing Normal University), we obtained the sequence of MLL1 PHD3-Bromo (1566−1784, Table S1) in a plasmid derived from the pGEX-6p-1 vector, tagged with GST at the N-terminus and 6xHis at the C-terminus.[9] To incorporate the UAA of 4-azido-L-phenylalanine (AzF) (Cat#: 34670-43-4, MedChemExpress, USA) into PHD3-Bromo (Figure S1), we used an orthogonal pair of aminoacyl tRNA synthetase/tRNA encoded in the pEVOL-pAzF plasmid (Cat#: 31186, Addgene, USA).[27,46] For the site-directed mutagenesis in PHD3-Bromo, we mutated a codon of the targeted amino acid to an amber stop codon (TAG)[46] using a kit of Hieff Mut (Cat#: 11003ES10, Yeasen Biotech, China).

We next expressed and purified the MLL1 PHD3-Bromo domain with AzF. We transformed two plasmids, mutated PHD3-Bromo and the tRNA synthetase/$tRNA_{CUA}$ pair, into *Escherichia coli* of BL21 (DE3), which were cultured in an adapted LB (2% of tryptone, 1% of yeast extract, and 1% of NaCI, pH 7.5) with ampicillin (100 μg/mL) and chloramphenicol (25 μg/mL) at 37 °C until OD_{600} reached 0.6−0.8. We supplemented the medium with a mixture (0.5 mM of isopropyl-β-D-1-thiogalactopyranoside (IPTG), 0.1 mM of zinc chloride ($ZnCl_2$), 0.2% of L-arabinose (w/v), and 1 mM of AzF). PHD fingers require Zn ions to fold correctly. After shaking at 30 °C for 16 h, we harvested cells which were further lysed using ultrasonic cell crusher (Scientz-IID, SCIENTZ, China) in a PBS buffer (pH 7.4). After centrifugation, we ran the supernatant through the resin (Cat#: 17531806, Ni Sepharose 6 Fast Flow, GE Healthcare, USA) which is capable of binding 6xHis tags, followed by extensive washing with imidazole (20 mM). We eluted our protein with an elution buffer containing imidazole at a linear gradient (50−300 mM). We then changed the elution buffer to PBS using Amicon Ultra centrifugal filter units (Cat#: UFC903024, Millipore, USA). We used the resin (Cat#: 17075601, GE) to bind our protein via GST tags, which were later removed by HRV 3C protease (Cat#: 88946, Thermo Fisher, USA). The final product of PHD3-Bromo with AzF (300−500 μM) was stored at −80 °C. We validated the expression and purification of PHD3-Bromo with AzF using SDS-Polyacrylamide gel electrophoresis (PAGE) and Western blots (Anti-6xHis tag, Cat#: ab9108, Abcam, USA).

Mass Spectrometry. We prepared a solution of the protein of interest which was infused at a flow rate of 5 μL/min into an autosampler for electrospray ionization. A MassPREP online desalting cartridge (Waters, USA) removed salts from the sample. We analyzed the desalted sample on a Q-TOF mass spectrometry (SYNAPT G2-Si, Waters, USA) with optimized conditions for large-mass proteins. We ran the measurements at 3 kV with data collected over the m/z range of 500−2000. Deconvoluted by MaxEnt 1 (Waters, USA), raw native electrospray mass spectra gave a spectrum (relative intensity versus mass) where all the charge-state peaks of individual species have collapsed into a single peak (zero-charge).

Bioconjugation between Proteins and DNA Using Copper-Free Click Chemistry. We used copper-free click chemistry of a strain-promoted alkyne−azide cycloaddition (SPAAC) to conjugate proteins and DNA oligos under physiological conditions in which the dibenzocyclooctyne group (DBCO) does not react with hydroxyls or amines. The setup of the click reaction was initiated by mixing the DBCO oligo (P^{DBCO} in Table S2, General Biosystems, Inc.) and the

DOI: 10.1021/acs.bioconjchem.9b00665
Bioconjugate Chem. 2019, 30, 2998−3006

azide-modified PHD3-Bromo at a molar ratio of 3:1 (0.15 mM vs 0.05 mM) in 10 μL of PBS (pH 7.4), avoiding light and shaking for 10 h at room temperature. PAGE stained by SYBR Green and SYPRO Ruby (Cat#: E33075, Thermo) revealed the final conjugate of protein−DNA. After separation of the reaction mixture using PAGE, we cut out the band containing the protein−DNA conjugate. To recover the conjugate from the gel piece, we used electroelution with D-tube Dialyzer (Cat#: 71506-3, MWCO = 3.5 kDa, Millipore, US),[47] followed by buffer change using Amicon filter (Cat#: UFC903024, Millipore, USA). The purified protein−DNA conjugate was stored in PBS at −20 °C.

Using the same methods above, we prepared the conjugate of peptide−DNA by performing the click reaction for DBCO modified DNA oligo (H^{DBCO} in Table S2, General Biosystems, Inc.) and azide-modified H3K4me3 peptide (Shanghai Top-Peptide Biotechnology, China) at a molar ratio of 2:3 (0.4 mM vs 0.6 mM).

Preparation of the PPI Construct for Single-Molecule Assays. Although following the same design, we have used different DNA primers to prepare handles, linkers, and anchors for the PPI construct. We next explained the plan using the materials for the H-tagged PPI construct as an example.

We used Cu(I)-catalyzed azide−alkyne cycloaddition (CuAAC) to make bifurcated conjugates of DNA oligos. If not explicitly noted, from Sangon Biotech we purchased all the azide and alkyne modified DNA oligos which were HPLC purified (Table S2). A typical recipe of click reaction has both an alkyne-DNA oligo (P^{Alkyne} or H^{Alkyne}) and an azide-DNA oligo (P^{Azide} or H^{Azide}) at 0.1 mM in 50 μL solution containing 10 mM of tris[(1-benzyl-1*H*-1,2,3-triazol-4-yl)methyl]amine (TBTA), 20 mM of sodium ascorbate and 2.5 mM of $CuSO_4$ (Figure S2). The reaction ran on a rotary shaker (220 rpm) at 25 °C avoiding light. After 1 h, we supplemented the reaction with 5 μL of TBTA at 100 mM, 2.5 μL of $CuSO_4$ at 50 mM, and 6.2 μL of sodium ascorbate at 160 mM. The reaction continued for another 3 h. We terminated the reaction by adding 1 μL of EDTA at 500 mM. We separated and purified the bifurcated conjugates of DNA oligos ($P^{\perp}$ or $H^{\perp}$) using denaturing urea PAGE in a buffer of 0.5× TBE. After ethanol precipitation, the bifurcated primers were recovered and stored at −20 °C.

We ran branched PCR to make dsDNA handles for the PPI construct. Fragments of λ-DNA served as PCR templates, which we validated to be no interactions with MLL1 PHD3-Bromo using electrophoretic mobility shift assay. The PCR used bifurcated primers ($P^{\perp}$ or $H^{\perp}$) and paired primers with attachment chemistry modifications (P^{Biotin} or $H^{Digoxigenin}$ in Table S2), producing biotin or digoxigenin handles of dsDNA with P^{Azide} or H^{Azide} branching out, respectively. We phosphorylated the oligo of the protein−DNA conjugates using T4 PNK. At 1:1:1 molar ratio, we annealed the biotin handle with DNA oligo of P^{Splint} (Table S2) and the protein−DNA conjugate of PHD3-Bromo-P^{DBCO} by heating to 65 °C and slowly cooling down to 4 °C. The nick at the branched DNA was ligated using T4 DNA ligase. We ran electrophoresis to obtain agarose gel containing the biotin handle of dsDNA with PHD3-Bromo, which was further isolated from the gel piece by electroelution in a dialysis bag. We changed the buffer and concentrated the product using an Amicon filter. We used the same protocol to prepare the digoxigenin handle with H3K4me3 using H^{Splint} (Table S2). The flexible linker of dsDNA was made by a regular PCR with primers L^F and L^R (Table S2). We ran three-piece ligation of the dsDNA handles and the flexible linker using T4 DNA ligase at the restriction sites of *BbvcI* and *BssSa I*. We collected the final PPI construct using agarose gel electrophoresis followed by gel cutting, electroelution, and Amicon filter to change buffer as steps above. The PPI construct was in a buffer of 10 mM Tris (pH 8) with 100 mM NaCl, stored at −80 °C.

Imaging of the PPI Construct Using an Atomic Force Microscope. To prepare the sample for imaging on an atomic force microscope (AFM), we generally mixed 20 μL of the PPI construct with 20 μL of $NiCl_2$ (4 mM) at room temperature, allowing 30 s without disturbance. We next loaded the sample on a freshly cleaved surface of mica, allowing 30 s for the PPI construct to bind the mica surface via Ni^{2+}. We then washed the unbinding sample away using water and dried the mica surface using nitrogen gas.

The experimental conditions of AFM were similar to the previous publication.[48] In brief, we examined the PPI construct in the air on a commercial AFM (JPK, Nanowizard II, Germany). We used cantilevers by Olympus (k = 26 N/m, OMCL-AC160TS-R3, Japan) or Bruker (k = 40 N/m, RTESPA-300, US). After aligning the laser, we used lambda DNA as a control sample to search for the best resonance frequency for AFM imaging. We used the tapping mode of AFM with the scanning line rate of 1 Hz. The resulting images were in a size of 512 × 512 pixels. We analyzed the pictures in the commercial software coming together with the AFM machine or in ImageJ (NIH Image, US).

Magnetic Tweezers. We have used a setup of homemade magnetic tweezers, similar to the one previously described,[29,49] which contain microscopy, motor-controlling magnets, Piezo stages, and a flow cell connecting to a pump. The inverted microscopy had an oil immersion objective (UPLFLN 100 × O2, Numerical aperture (N.A.) = 1.3; Olympus, Japan) and a tube lens (Cat#: AC508-400-A, f = 400 mm, Thorlabs, USA) resulting in magnification of 222×. Image collection was by a CMOS camera (Cat#: MC1362, Mikrotron, Germany), a frame grabber device of PCIe 1433 (National Instruments, USA) and Camera Link cables. Collected images went to a CUDA supporting graphics card of GeForce GTX 745 (NVIDIA, USA) and a CPU of Intel Core i7−6700 (Intel, USA) for further analysis in a desktop computer supported by Windows 10 (64-bit). A pair of NdFeB magnets (Cat#: W-05-N50-G, Webcraft GmBH, Germany) was vertically aligned to generate a strong magnetic field. A gap of 1 mm between two magnets allowed illumination from a 660 nm LED (Cat#: M660F1, Thorlabs). A translate stage (Cat#: M-404.1PD, Physik Instrumente, Germany) controlled the magnets in the vertical direction while a rotary motor (Cat#: C-150.PD, Physik Instrumente) rotated the magnets in the xy-plane. A piezo nanopositioner (Cat#: P-726.1CD, Physik Instrumente) could precisely move the objective in the z-direction. A flow cell with a single channel was made of two coverslips (Cat#: S1699-12-100EA, i-Quip, USA) and double layers of parafilm with the channel connected to a peristaltic pump (Cat#: ISM832, Ismatec, Germany).

We used a custom-written application in Labview 2017, which served as a user interface in magnetic tweezers to configure hardware, set up experiments, and analyze data, similar to that published in the literature.[50] A Quadrant Interpolation algorithm in this application can accurately and simultaneously analyze video-based images of microspheres. A

DOI: 10.1021/acs.bioconjchem.9b00665
Bioconjugate Chem. 2019, 30, 2998−3006

CUDA parallel computing framework can track microspheres and extract *xyz* coordinates in real time.

Single-Molecule Assays Using Magnetic Tweezers. We performed single-molecule experiments base on a setup of microsphere-DNA-coverslip in a microfluidic chamber. Routinely, we mixed 0.1 ng of DNA−protein construct with 10 μL of streptavidin-coated microspheres (Cat#: 65305, M270, Invitrogen, USA) in 40 μL of PBS buffer (pH 7.4) or Tris buffer (pH 8.0, 10 mM Tris, 100 mM NaCl). We incubated anti-digoxigenin antibody (0.1 mg/mL) for 2−4 h on top of a matrix of nitrocellulose (0.1%, m/v) on a coverslip which was later passivated with BSA (5 mg/mL) overnight. DNA molecules were immobilized between the coverslip surface and the microspheres. We ran force-ramp assays at 200 Hz of the sampling rate in a PBS buffer (pH 7.4), or a Tris buffer (pH 8.0), supplemented with 10 μM of $ZnCl_2$ and 0.00315% Tween 20.

Other than explicitly stated, we used Matlab 2017b (MathWorks, USA) to analyze data. We applied a modified Marko-Siggia Worm-Like-Chain model[51,52] to examine the traces of force (F) and extension (x)

$$F = \left(\frac{k_B T}{L_p}\right)\left[\frac{1}{4\left(1 - \frac{x}{L_0} + \frac{F}{S}\right)^2} - \frac{1}{4} + \frac{x}{L_0} - \frac{F}{S}\right] \quad (1)$$

where L_p is the persistence length, L_0 is the contour length, S is the stretch modulus, $k_B T$ stands for that Boltzmann's constant times temperature.

■ ASSOCIATED CONTENT

Supporting Information

The Supporting Information is available free of charge on the ACS Publications website at DOI: 10.1021/acs.bioconjchem.9b00665.

Protein sequences, Oligodeoxynucleotides, Scheme for genetic incorporation of UAA, Preparation of bifurcated ssDNA, Incorporation of UAA into the PHD3-Bromo domain of MLL1, Bioconjugation of PHD3-Bromo and DNA (PDF)

■ AUTHOR INFORMATION

Corresponding Authors

*E-mail: zyu@nankai.edu.cn.
*E-mail: zhangwk@jlu.edu.cn.
*E-mail: junhuchen@hotmail.com.

ORCID

Wenke Zhang: 0000-0002-4569-6035
Zhongbo Yu: 0000-0002-0634-554X

Notes

The authors declare no competing financial interest.

■ ACKNOWLEDGMENTS

We thank Dr. Zhanxin Wang (Beijing Normal University) for the plasmid of PHD3-Bromo, Dr. Eugen Stulz (University of Southampton), Dr. D. Dafydd Jones (Cardiff University), and Gabriella Marth (University of Southampton) for constructive discussion in the optimization of UAA mutagenesis. This work was supported by the Fundamental Research Funds for the Central Universities, Nankai University [035-63161138, 035-63191141, and 035-63191735 to Z. Y.]. We also acknowledge support from National Natural Science Foundation of China [Grants 31670763 to Z. Y. and 81101266 to J. C.], Natural Science Foundation of Tianjin of China [Grant 15JCZDJC65400 to Z. Y.], and the Project of Shanghai Science and Technology Commission (Grant No. 18490741100 to J. C.). Funding for open access charge: National Natural Science Foundation of China.

■ REFERENCES

(1) Corbi-Verge, C., Garton, M., Nim, S., and Kim, P. M. (2017) Strategies to Develop Inhibitors of Motif-Mediated Protein-Protein Interactions as Drug Leads. *Annu. Rev. Pharmacol. Toxicol. 57*, 39−60.

(2) Scott, D. E., Bayly, A. R., Abell, C., and Skidmore, J. (2016) Small molecules, big targets: drug discovery faces the protein-protein interaction challenge. *Nat. Rev. Drug Discovery 15*, 533−550.

(3) Otten, M., Ott, W., Jobst, M. A., Milles, L. F., Verdorfer, T., Pippig, D. A., Nash, M. A., and Gaub, H. E. (2014) From genes to protein mechanics on a chip. *Nat. Methods 11*, 1127−1130.

(4) Verdorfer, T., Bernardi, R. C., Meinhold, A., Ott, W., Luthey-Schulten, Z., Nash, M. A., and Gaub, H. E. (2017) Combining in Vitro and in Silico Single-Molecule Force Spectroscopy to Characterize and Tune Cellulosomal Scaffoldin Mechanics. *J. Am. Chem. Soc. 139*, 17841−17852.

(5) Bertz, M., Buchner, J., and Rief, M. (2013) Mechanical stability of the antibody domain CH3 homodimer in different oxidation states. *J. Am. Chem. Soc. 135*, 15085−15091.

(6) Spadaro, D., Le, S., Laroche, T., Mean, I., Jond, L., Yan, J., and Citi, S. (2017) Tension-Dependent Stretching Activates ZO-1 to Control the Junctional Localization of Its Interactors. *Current biology. Curr. Biol. 27*, 3783−3795.

(7) Le, S., Hu, X., Yao, M., Chen, H., Yu, M., Xu, X., Nakazawa, N., Margadant, F. M., Sheetz, M. P., and Yan, J. (2017) Mechanotransmission and Mechanosensing of Human alpha-Actinin 1. *Cell Rep. 21*, 2714−2723.

(8) Vera, A. M., and Carrion-Vazquez, M. (2016) Direct Identification of Protein-Protein Interactions by Single-Molecule Force Spectroscopy. *Angew. Chem., Int. Ed. 55*, 13970−13973.

(9) Wang, Z., Song, J., Milne, T. A., Wang, G. G., Li, H., Allis, C. D., and Patel, D. J. (2010) Pro isomerization in MLL1 PHD3-bromo cassette connects H3K4me readout to CyP33 and HDAC-mediated repression. *Cell 141*, 1183−1194.

(10) Zhang, G., Smith, S. G., and Zhou, M. M. (2015) Discovery of Chemical Inhibitors of Human Bromodomains. *Chem. Rev. 115*, 11625−11668.

(11) Dawson, M. A. (2017) The cancer epigenome: Concepts, challenges, and therapeutic opportunities. *Science 355*, 1147−1152.

(12) Erfurth, F. E., Popovic, R., Grembecka, J., Cierpicki, T., Theisler, C., Xia, Z. B., Stuart, T., Diaz, M. O., Bushweller, J. H., and Zeleznik-Le, N. J. (2008) MLL protects CpG clusters from methylation within the Hoxa9 gene, maintaining transcript expression. *Proc. Natl. Acad. Sci. U. S. A. 105*, 7517−7522.

(13) Cierpicki, T., Risner, L. E., Grembecka, J., Lukasik, S. M., Popovic, R., Omonkowska, M., Shultis, D. D., Zeleznik-Le, N. J., and Bushweller, J. H. (2010) Structure of the MLL CXXC domain-DNA complex and its functional role in MLL-AF9 leukemia. *Nat. Struct. Mol. Biol. 17*, 62−68.

(14) Li, M., Xia, X., Tian, Y., Jia, Q., Liu, X., Lu, Y., Li, M., Li, X., and Chen, Z. (2019) Mechanism of DNA translocation underlying chromatin remodelling by Snf2. *Nature 567*, 409−413.

(15) Chen, P., Dong, L., Hu, M., Wang, Y. Z., Xiao, X., Zhao, Z., Yan, J., Wang, P. Y., Reinberg, D., Li, M., et al. (2018) Functions of FACT in Breaking the Nucleosome and Maintaining Its Integrity at the Single-Nucleosome Level. *Mol. Cell 71*, 284−293.

(16) Lavelle, C., Praly, E., Bensimon, D., Le Cam, E., and Croquette, V. (2011) Nucleosome-remodelling machines and other molecular motors observed at the single-molecule level. *FEBS J. 278*, 3596−3607.

DOI: 10.1021/acs.bioconjchem.9b00665
Bioconjugate Chem. 2019, 30, 2998−3006

(17) Ngo, T. T., Zhang, Q., Zhou, R., Yodh, J. G., and Ha, T. (2015) Asymmetric unwrapping of nucleosomes under tension directed by DNA local flexibility. *Cell 160*, 1135−1144.
(18) Deindl, S., Hwang, W. L., Hota, S. K., Blosser, T. R., Prasad, P., Bartholomew, B., and Zhuang, X. (2013) ISWI remodelers slide nucleosomes with coordinated multi-base-pair entry steps and single-base-pair exit steps. *Cell 152*, 442−452.
(19) Vlijm, R., Lee, M., Lipfert, J., Lusser, A., Dekker, C., and Dekker, N. H. (2015) Nucleosome assembly dynamics involve spontaneous fluctuations in the handedness of tetrasomes. *Cell Rep. 10*, 216−225.
(20) Reddington, S. C., Tippmann, E. M., and Jones, D. D. (2012) Residue choice defines efficiency and influence of bioorthogonal protein modification via genetically encoded strain promoted Click chemistry. *Chem. Commun. 48*, 8419−8421.
(21) Marth, G., Hartley, A. M., Reddington, S. C., Sargisson, L. L., Parcollet, M., Dunn, K. E., Jones, D. D., and Stulz, E. (2017) Precision Templated Bottom-Up Multiprotein Nanoassembly through Defined Click Chemistry Linkage to DNA. *ACS Nano 11*, 5003−5010.
(22) Vulliez-Le Normand, B., Tonkin, M. L., Lamarque, M. H., Langer, S., Hoos, S., Roques, M., Saul, F. A., Faber, B. W., Bentley, G. A., Boulanger, M. J., et al. (2012) Structural and Functional Insights into the Malaria Parasite Moving Junction Complex. *PLoS Pathog. 8*, No. e1002755.
(23) Xiang, Z., Lacey, V. K., Ren, H., Xu, J., Burban, D. J., Jennings, P. A., and Wang, L. (2014) Proximity-enabled protein crosslinking through genetically encoding haloalkane unnatural amino acids. *Angew. Chem., Int. Ed. 53*, 2190−2193.
(24) Brustad, E. M., Lemke, E. A., Schultz, P. G., and Deniz, A. A. (2008) A general and efficient method for the site-specific dual-labeling of proteins for single molecule fluorescence resonance energy transfer. *J. Am. Chem. Soc. 130*, 17664−17665.
(25) Pokhrel, N., Origanti, S., Davenport, E. P., Gandhi, D., Kaniecki, K., Mehl, R. A., Greene, E. C., Dockendorff, C., and Antony, E. (2017) Monitoring Replication Protein A (RPA) dynamics in homologous recombination through site-specific incorporation of non-canonical amino acids. *Nucleic Acids Res. 45*, 9413−9426.
(26) Liu, C. C., and Schultz, P. G. (2010) Adding new chemistries to the genetic code. *Annu. Rev. Biochem. 79*, 413−444.
(27) Ryu, Y., and Schultz, P. G. (2006) Efficient incorporation of unnatural amino acids into proteins in Escherichia coli. *Nat. Methods 3*, 263−265.
(28) Yang, Z., and Champoux, J. J. (2009) In *DNA Topoisomerases: Methods and Protocols* (Clarke, D. J., Ed.) pp 49−57, Humana Press, Totowa, NJ.
(29) Li, N., Wang, J., Ma, K., Liang, L., Mi, L., Huang, W., Ma, X., Wang, Z., Zheng, W., Xu, L., et al. (2019) The dynamics of forming a triplex in an artificial telomere inferred by DNA mechanics. *Nucleic Acids Res. 47*, e86−e86.
(30) Morfill, J., Kuhner, F., Blank, K., Lugmaier, R. A., Sedlmair, J., and Gaub, H. E. (2007) B-S transition in short oligonucleotides. *Biophys. J. 93*, 2400−2409.
(31) Khanal, A., Long, F., Cao, B., Shahbazian-Yassar, R., and Fang, S. (2016) Evidence of Splitting 1,2,3-Triazole into an Alkyne and Azide by Low Mechanical Force in the Presence of Other Covalent Bonds. *Chem. - Eur. J. 22*, 9760−9767.
(32) Kolb, H. C., Finn, M. G., and Sharpless, K. B. (2001) Click Chemistry: Diverse Chemical Function from a Few Good Reactions. *Angew. Chem., Int. Ed. 40*, 2004−2021.
(33) Meldal, M., and Tornoe, C. W. (2008) Cu-catalyzed azide-alkyne cycloaddition. *Chem. Rev. 108*, 2952−3015.
(34) Yu, Z., Cui, Y., Selvam, S., Ghimire, C., and Mao, H. (2015) Dissecting cooperative communications in a protein with a high-throughput single-molecule scalpel. *ChemPhysChem 16*, 223−232.
(35) Yu, Z., Koirala, D., Cui, Y., Easterling, L. F., Zhao, Y., and Mao, H. (2012) Click chemistry assisted single-molecule fingerprinting reveals a 3D biomolecular folding funnel. *J. Am. Chem. Soc. 134*, 12338−12341.
(36) Selvam, S., Yu, Z., and Mao, H. (2016) Exploded view of higher order G-quadruplex structures through click-chemistry assisted single-molecule mechanical unfolding. *Nucleic Acids Res. 44*, 45−55.
(37) Walder, R., LeBlanc, M. A., Van Patten, W. J., Edwards, D. T., Greenberg, J. A., Adhikari, A., Okoniewski, S. R., Sullan, R. M. A., Rabuka, D., Sousa, M. C., et al. (2017) Rapid Characterization of a Mechanically Labile alpha-Helical Protein Enabled by Efficient Site-Specific Bioconjugation. *J. Am. Chem. Soc. 139*, 9867−9875.
(38) Stigler, J., Ziegler, F., Gieseke, A., Gebhardt, J. C., and Rief, M. (2011) The complex folding network of single calmodulin molecules. *Science 334*, 512−516.
(39) Shank, E. A., Cecconi, C., Dill, J. W., Marqusee, S., and Bustamante, C. (2010) The folding cooperativity of a protein is controlled by its chain topology. *Nature 465*, 637−640.
(40) Dietz, H., and Rief, M. (2006) Protein structure by mechanical triangulation. *Proc. Natl. Acad. Sci. U. S. A. 103*, 1244−1247.
(41) Kilchherr, F., Wachauf, C., Pelz, B., Rief, M., Zacharias, M., and Dietz, H. (2016) Single-molecule dissection of stacking forces in DNA. *Science 353*, aaf5508.
(42) Lin, W., Ma, J., Nong, D., Xu, C., Zhang, B., Li, J., Jia, Q., Dou, S., Ye, F., Xi, X., et al. (2017) Helicase Stepping Investigated with One-Nucleotide Resolution Fluorescence Resonance Energy Transfer. *Phys. Rev. Lett. 119*, 138102.
(43) Ranjith, P., Yan, J., and Marko, J. F. (2007) Nucleosome hopping and sliding kinetics determined from dynamics of single chromatin fibers in Xenopus egg extracts. *Proc. Natl. Acad. Sci. U. S. A. 104*, 13649−13654.
(44) Mollazadeh-Beidokhti, L., Mohammad-Rafiee, F., and Schiessel, H. (2012) Nucleosome dynamics between tension-induced states. *Biophys. J. 102*, 2235−2240.
(45) Shundrovsky, A., Smith, C. L., Lis, J. T., Peterson, C. L., and Wang, M. D. (2006) Probing SWI/SNF remodeling of the nucleosome by unzipping single DNA molecules. *Nat. Struct. Mol. Biol. 13*, 549−554.
(46) Chin, J. W., Santoro, S. W., Martin, A. B., King, D. S., Wang, L., and Schultz, P. G. (2002) Addition of p-azido-L-phenylalanine to the genetic code of Escherichia coli. *J. Am. Chem. Soc. 124*, 9026−9027.
(47) Sambrook, J., and Russell, D. W. (2006) Recovery of DNA from agarose and polyacrylamide gels: electroelution into dialysis bags. *CSH protocols 2006*, pdb.prot4023.
(48) Liu, J., Wang, X., and Zhang, W. (2018) Atomic Force Microscopy Imaging Study of Aligning DNA by Dumbbell-like Au-Fe3O4Magnetic Nanoparticles. *Langmuir 34*, 14875−14881.
(49) Yu, Z., Dulin, D., Cnossen, J., Kober, M., van Oene, M. M., Ordu, O., Berghuis, B. A., Hensgens, T., Lipfert, J., and Dekker, N. H. (2014) A force calibration standard for magnetic tweezers. *Rev. Sci. Instrum. 85*, 123114.
(50) Cnossen, J. P., Dulin, D., and Dekker, N. H. (2014) An optimized software framework for real-time, high-throughput tracking of spherical beads. *Rev. Sci. Instrum. 85*, 103712.
(51) Wang, M. D., Yin, H., Landick, R., Gelles, J., and Block, S. M. (1997) Stretching DNA with optical tweezers. *Biophys. J. 72*, 1335−1346.
(52) Marko, J. F., and Siggia, E. D. (1995) Stretching DNA. *Macromolecules 28*, 8759−8770.

DOI: 10.1021/acs.bioconjchem.9b00665
Bioconjugate Chem. 2019, 30, 2998−3006